



The census of dense cores in the Serpens region from the Herschel Gould Belt Survey

Eleonora Fiorellino^{1,2,3,4,5}, D. Elia³, P. André⁶, A. Men'shchikov⁶, S. Pezzuto³, E. Schisano³, M. Benedettini³, V. Konyves⁶, J. Kirk⁷, S. Bontemps^{8,9}, J. Di Francesco^{10,11}, F. Motte¹²

¹ Università di Roma Tor Vergata, Rome, Italy; ² Università di Roma La Sapienza, Rome, Italy; ³ INAF – IAPS, Rome, Italy; ⁴ INAF – OAR, Rome, Italy; ⁵ ESO, Garching bei Munchen, Germany; ⁶ AIM, CEA/DSM-CNRS-Université Paris Diderot, IRFU/Service d'Astrophysique, Saclay, France; ⁷ University of Warwick, Coventry, UK; ⁸ Univ. Bordeaux, Floirac, France; ⁹ CNRS, Floirac, France; ¹⁰ University of Victoria, Victoria, Canada; ¹¹ NRCC, Victoria, Canada; ¹² University Grenoble Alpes, CNRS, IPAG, Grenoble, France

The Serpens region

The Serpens region was recognized as a star formation site by Strom et al. (1974). It extends over several square degrees around the variable star VV-Ser and it is part of the Aquila Rift cloud complex. It is a young complex (around 2 Myr, Enoch et al. 2008), in which are present both Young Stellar Objects (YSOs) and prestellar cores. For this reason and because of its nearness, ($d = 436$ pc, Ortiz-Leon et al. 2018), this region is one of the most studied. Serpens is one of the targets of the Herschel Gould Belt Survey (HGBS) project which observed the main star-forming regions within 500 pc. Herschel, however, observed in the far-IR at 70 and 160 μm with PACS instrument and at 250, 350 and 500 μm with SPIRE instrument. The most studied part of the Serpens cloud is named Serpens Main, Herschel satellite observed a wider region, contained in the blue box in Fig. 1, compared to the region usually considered in literature, which corresponds to the green box in Fig. 1. Serpens Main is situated very close to the Aquila Rift, in the Milky Way's mid-plane. Our observations include also a portion of the easternmost Aquila Rift, the red box in Fig. 1. The Serpens star-forming region is also interesting because it is one of the first regions for which the Core Mass Function (CMF) was computed and compared to the stellar Initial Mass Function (IMF), finding a good agreement in slope at high masses (Testi & Sargent, 1998). Here we report the main Serpens features as obtained from Herschel observations: the column density and dust temperature maps, the first complete census of cores and their relationship with the filamentary structure.

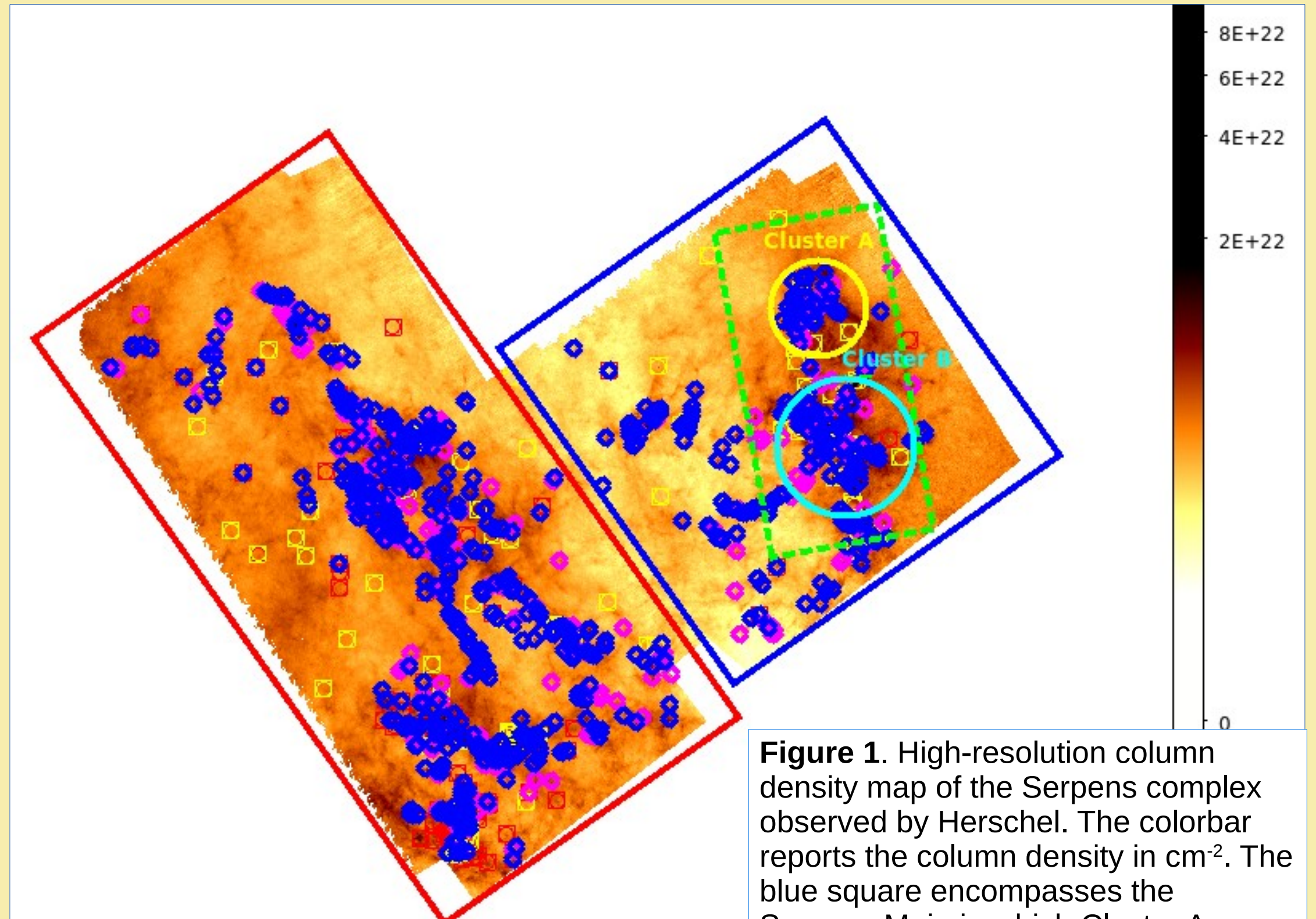
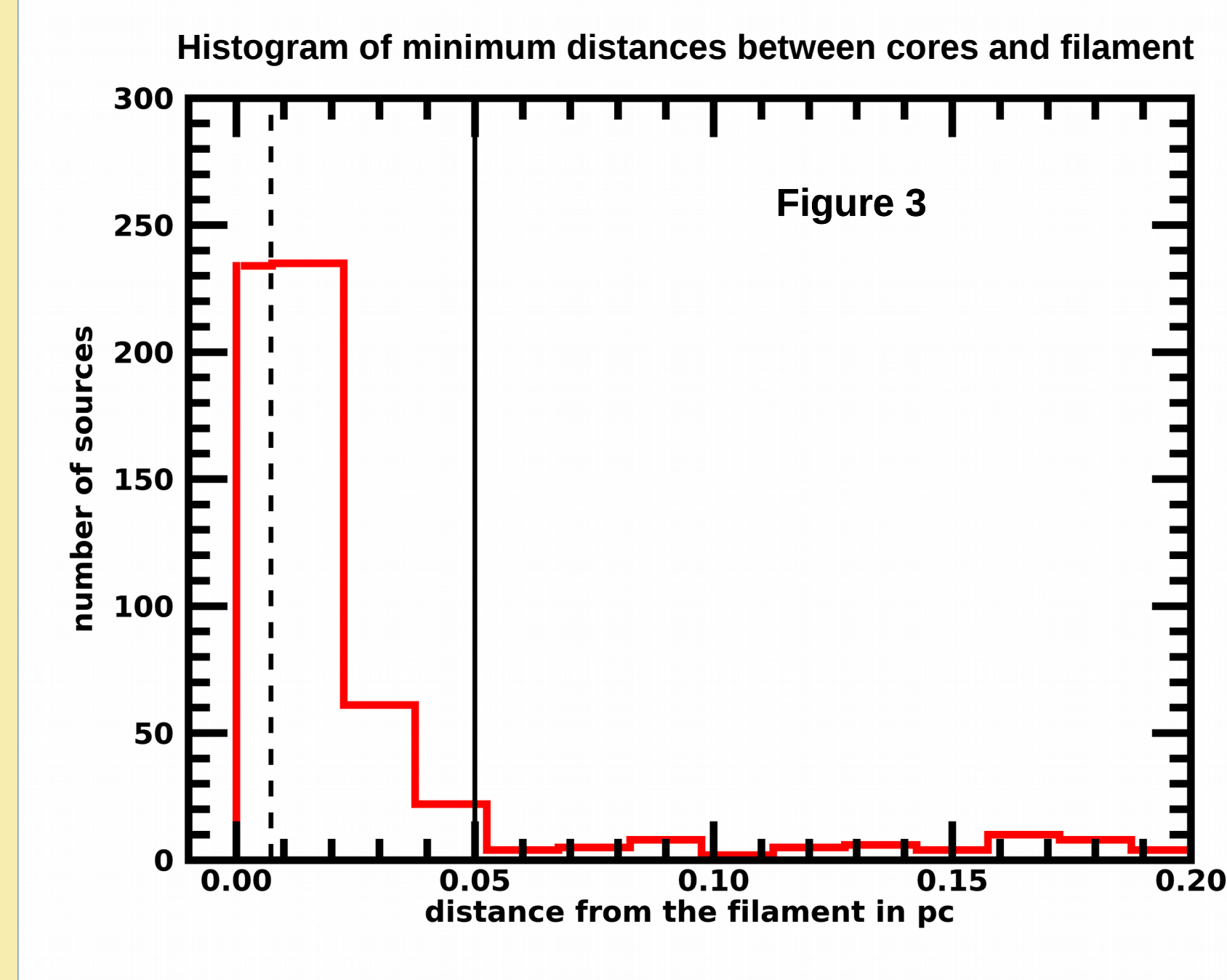
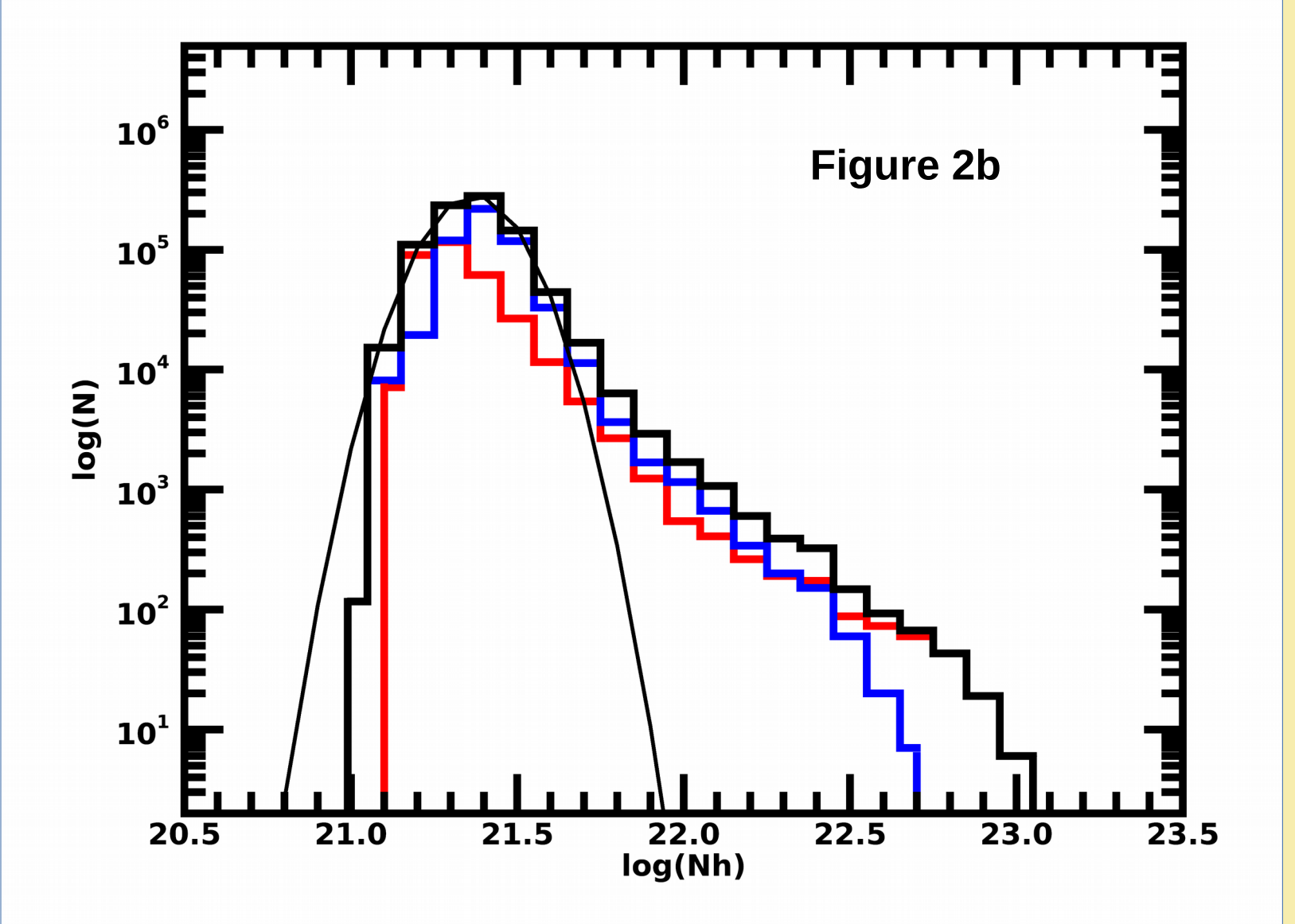
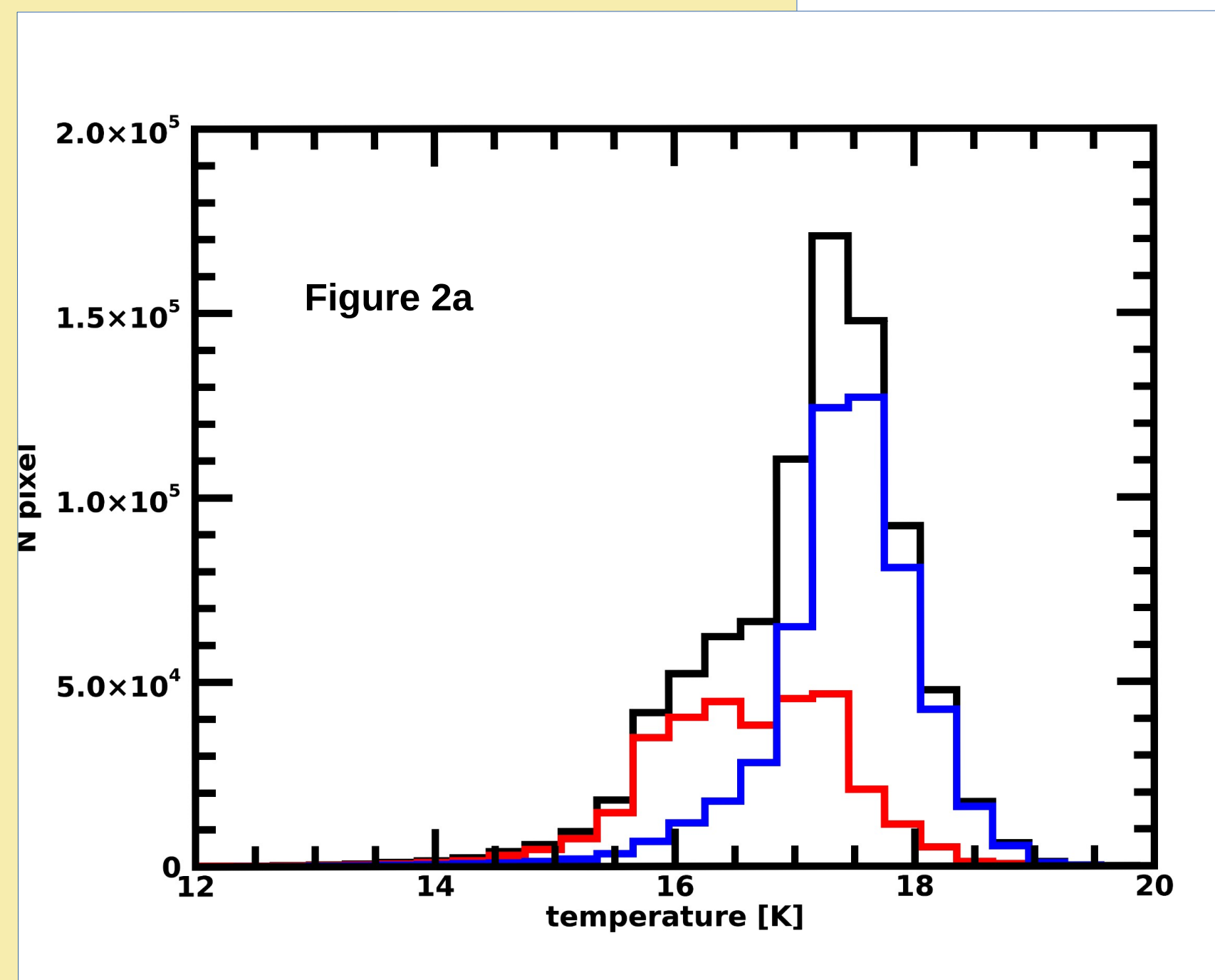


Figure 1. High-resolution column density map of the Serpens complex observed by Herschel. The colorbar reports the column density in cm^{-2} . The blue square encompasses the Serpens Main in which Cluster A (magenta circle) and Cluster B (cyan circle) are located (Djupvik et al. 2006; Harvey et al 2006; Levashakov et al. 2013); the red rectangle contains the Eastern part of the Aquila Rift. The green dashed box shows the part of the Serpens we select to compare our results about Serpens mass with the previous ones.

Column Density & Dust Temperature Maps

We assume that the interstellar dust emits in the far-IR as a modified blackbody. We adopt $d=436$ pc for all the sources in the cloud (Ortiz-Léon et al. 2018). The temperature and column density maps were obtained pixel-by-pixel by fitting a modified black body to 160, 250, 350 and 500 μm fluxes, after re-projecting each map over the grid at 500 μm . The 70 μm map was not involved because the modified black body approximation is reliable for $\lambda \gg 100 \mu\text{m}$, while at shorter wavelengths the dust is not optically thin, and both cold and hot dust components are present. In Fig. 2a the temperature map is reported. The total distribution (black) shows a peak at about 17.5 K and a secondary bump at about 16.5 K, corresponding to the peaks of distributions for subregions: the highest at about 17.5 K, due to the Aquila Rift contribution (blue); the lowest at about 16.5 K, mostly due to the Serpens Main temperature distribution (red). In Fig. 2b the histogram of column density is shown. The main contribution to the peak, which lies at $2.5 \times 10^{21} \text{ cm}^{-2}$, is due to the Aquila Rift region while the peak of Serpens region is located at lower column density values (about $2 \times 10^{21} \text{ cm}^{-2}$). Integrating the column density map over the whole region we obtain a total mass of $49905 M_{\text{sun}}$ for HGBS Serpens. We compute the optical depth of the region with Herschel and Planck data, finding an agreement within 1σ : $\langle \tau_{\text{H}}/\tau_{\text{P}} \rangle = 0.98 \pm 0.39$. On the contrary, the mass we derive is higher than in previous works that considered the same region, also taking into account different distances adopted (White et al. 1995; McMullin et al. 2000; Olmi & Testi 2002; Nakamura et al. 2017). This is mainly due to the method: we fit a greybody function, they use spectroscopic tracers (^{12}CO , ^{13}CO , C^{18}O , C^{17}O).



Compact source detection and classification

Cores are roundish compact sources of about 0.1 pc in size, made of gas (99%) and dust (1%) which can eventually collapse forming protostars. From Herschel maps we extract the catalogue of dense cores. For uniformity with HGBS works, the catalogue is the result of an essentially two-step process, clearly described in Marsh et al. (2016): detection and classification. Source extraction is carried out by the multi-wavelength, multi-scale software GETSOURCES (Men'shchikov et al. 2012) which produces a preliminary version of starless core (detection between 160 and 500 μm) and protostellar core (detection at 70 μm) catalogue, i.e. those sources which are candidate to be class 0 objects. This list is filtered to select only reliable cores. Then it is matched with IR catalogues (WISE and Spitzer), to rule out from the catalogue those evolved YSOs which emit also at higher wavelengths, and with NED and Simbad, to avoid the presence of stars or galaxies. **We find 833 dense cores, of which 709 are starless and 124 protostellar.** Then, we fit a modified blackbody to their spectral energy distribution (SED) to determine, for each source, the mass and the temperature. This was possible for 594 sources, **77 of which are protostellar cores and 517 starless cores**, respectively. To determine the nature of a starless core, we use the Bonnor-Ebert criterion (BE): if the core mass is larger than the BE mass ($M_{\text{BE}} = 2.4 R_{\text{BE}} a_s^2 / G$), then the core is gravitationally bound, where R_{BE} is the radius of the core, $a_s^2 = kT/\mu m_{\text{H}}$ is the isothermal sound speed and G is the gravitational constant. Further relaxing the boundness criterion as in Konyves et al. 2015, we find **374 robust prestellar cores and 53 tentative prestellar ones.**

References

- Chabrier et al. 2005, A&SSL Vol. 327, 41
- Enoch et al. 2008, ApJ, 684, 1240
- Konyves et al. 2015, A&A, 584, A91
- Kramer et al. 1998, A&A, 329, 249
- Kroupa 2001, MNRAS, 322, 231
- Marsh et al. 2016, MNRAS, 459, 342
- McMullin et al. 200, ApJ, 536, 845
- Men'shchikov et al 2012, A&A, 542, A81
- Nakamura et al. 2017, ApJ, 837, 154
- Olmi & Testi 2002, A&A, 392, 1053
- Ortiz-Léon et al. 2018, ApJ, 869, L33
- Salpeter 1995, ApJ, 121, 161
- Schisano et al. 2014, ApJ, 791, 27
- Sewilo et al. 2019, ApJS, 240, 26S
- Testi & Sargent 1998, ApJ, 508, L91
- White et al. 1995, A&A, 298, 594

The relation between cores and filamentary structure

In order to detect and characterize the sources lying on filaments, we performed a filament detection on the column density map on the column density map the algorithm presented in Schisano et al. (2014), which uses the eigenvalues of the Hessian matrix of a map. We first consider that a source is spatially associated with a filament if its central position falls within the boundary of the filament, as it is evaluated by the algorithm. Following this method we find that 68.9% of the entire catalogue sources are on filaments. We decide to provide a further definition of source/filaments spatial association, inspired by the analysis of Sewilo et al (2019) for associating YSOs to nearest filaments, based on the minimum distance between the two. From the histogram of these distances (Fig. 3) it can be noticed that there is a remarkable amount of cores near the spine of the filament, while for larger distances associated sources are more sparse. **We decide to associate a source to a filament if it is contained in the first group near the spine which corresponds to a maximum distance from the filament of 0.05 pc, which is in turn compatible with the typical size of filaments in GB regions, based on previous Herschel observations, of about 0.1 pc** (André 2014). We find that the **66.3% of the sources are on-filament**, according with this definition. This result seems to be in agreement with the scenario in which filaments play a fundamental role in star formation, being probably the sites in which cores form and an intermediate step between the fragmentation of molecular clouds and the collapse of cores.

The Core Mass Function

We computed the core mass function (CMF) of robust prestellar, candidate prestellar and unbound cores which are shown as a blue, a light blue and a green solid line, respectively, in Fig. 4. **Both unbound and prestellar CMF are well fitted by a lognormal function** (red and dashed red line, respectively) **up to the turn around, which is at about $3 M_{\text{sun}}$** . At higher masses the prestellar CMF shape follows a power-law, with slope -1.2 ± 0.5 (solid thick dark line). For comparison, the CO clumps mass function (Kramer et al. 1998), the Kroupa (2001) and Chabrier (2005) stellar IMFs are plotted in dotted, dashed and solid black, respectively. The blue dotted-dashed vertical line represents the mass completeness limit for prestellar sources. The power-law slope was already determined by Testi & Sargent (1998) and our result is in agreement with theirs. **This is the first time that we can observe also the lognormal part of the CMF shape for this region, thanks to the sensitivity of Herschel satellite.** Lognormal+power-law is exactly the shape of Salpeter's IMF, therefore the fact that we find such an agreement in shape between CMF and IMF supports the hypothesis of the strong correlation between the fragmentation process of molecular clouds which forms cores and statistical mass distribution of stars.

